FGF14 is a regulator of KCNQ2/3 channels

Juan Lorenzo Pablo[a,b] and Geoffrey S. Pitt[a,b,c,1,2]

[a]Department of Neurobiology, Duke University Medical Center, Durham, NC 27710; [b]Ion Channel Research Unit, Duke University Medical Center, Durham, NC 27710; and [c]Division of Cardiology, Department of Medicine, Duke University Medical Center, Durham, NC 27710

Edited by Richard W. Aldrich, University of Texas at Austin, Austin, TX, and approved December 1, 2016 (received for review June 22, 2016)

KCNQ2/3 (Kv7.2/7.3) channels and voltage-gated sodium channels (VGSCs) are enriched in the axon initial segment (AIS) where they bind to ankyrin-G and coregulate membrane potential in central nervous system neurons. The molecular mechanisms supporting coordinated regulation of KCNQ and VGSCs and the cellular mechanisms governing KCNQ trafficking to the AIS are incompletely understood. Here, we show that fibroblast growth factor 14 (FGF14), previously described as a VGSC regulator, also affects KCNQ function and localization. FGF14 knockdown leads to a reduction of KCNQ2 in the AIS and a reduction in whole-cell KCNQ currents. FGF14 positively regulates KCNQ2/3 channels in a simplified expression system. FGF14 interacts with KCNQ2 at a site distinct from the FGF14–VGSC interaction surface, thus enabling the bridging of $Na_V1.6$ and KCNQ2. These data implicate FGF14 as an organizer of channel localization in the AIS and provide insight into the coordination of KCNQ and VGSC conductances in the regulation of membrane potential.

FGF14 | KCNQ2 | fibroblast growth factor homologous factors | axon initial segment | ankyrin-G

Neurons express a wide diversity of ion channels and yet are able to target different channels specifically to cellular subcompartments such as the axon initial segment (AIS) (1, 2). Among the channels specifically targeted to the AIS are the voltage-gated sodium channels (VGSCs) and KCNQ2/3 (Kv7.2/Kv7.3) voltage-gated potassium channels (3–5). VGSCs are trapped in the AIS through binding to the scaffolding protein ankyrin-G (ank-G), which anchors transmembrane molecules to the spectrin–actin cytoskeleton (4, 6, 7). Localization of KCNQ2/3 channels of the K_V7 family to the AIS has been proposed to follow the model of VGSCs, because KCNQ2/3 channels contain the same ank-G binding motifs that trap VGSCs (8). Moreover, VGSCs and KCNQ2/3 channels both bind to the ankyrin repeats in ank-G, albeit at distinct but overlapping interaction sites (9, 10). However, other determinants for AIS localization outside of the ankyrin-binding motif have been described, thus pointing to additional modes of regulation (11–13).

The tight colocalization of K_V7 channels with VGSCs has been postulated to confer specific coregulatory properties. In the soma, dendrites, and AIS, K_V7 channels attenuate subthreshold depolarization by opposing a VGSC persistent current, whereas in the nodes, K_V7 channels stabilize the membrane potential and protect VGSC channels from inactivation (14). Although ank-G serves as an AIS anchor for both K_V7 channels and VGSCs, simultaneous binding of both channels to one ank-G molecule has not been demonstrated, and the molecular mechanisms underlying the coordination between Kv7 channels and VGSCs are incompletely understood. We hypothesized that fibroblast growth factor homologous factors (FHFs), a subfamily (FGF11–14) of fibroblast growth factors that function as intracellular modulators of VGSCs (15, 16) are candidate contributing factors. FHFs have been implicated in neurological diseases characterized by altered excitability, as exemplified by spinocerebellar ataxia 27 (SCA27) mutations in *FGF14* (17, 18). Because FGF14 interacts directly with VGSCs, *FGF14* mutations have been postulated to cause disease through VGSC dysfunction. Nevertheless, the pathologic mechanisms may be broader, as FGF14 also regulates presynaptic voltage-gated Ca^{2+} channels (19). Whether the disease process extends beyond dysregulation of VGSCs and voltage-gated Ca^{2+} channels is not known.

Here, we focused on the neuronally restricted FGF14 because it is highly localized to the AIS, it binds directly to VGSCs, and protects them from inactivation (16, 20–24). We therefore reasoned that FGF14 might coordinate KCNQ2/3 channels and VGSCs in the AIS. We report that FGF14 is critical to the regulation of KCNQ2 channels in hippocampal neurons. FGF14 knockdown leads to a loss of KCNQ2 in the AIS and decreases KCNQ2/3 currents. VGSCs are not required for this regulation because FGF14 also increases KCNQ2/3 current in a heterologous expression system devoid of VGSCs. FGF14 interacts with KCNQ2 using an interface distinct from the well-defined VGSC binding site on FHFs. Thus, FGF14 can "bridge" VGSCs and KCNQ2. These data not only establish FGF14 as a regulator of KCNQ2 channels, but also show that FGF14 may be a broad organizer of AIS ion channels.

Results

Because of the restricted localization of FGF14 to the AIS and our recent data that FGF14 can regulate multiple ion channels, we first tested whether FGF14 also regulated the AIS-enriched KCNQ2 channels. We knocked down FGF14 in neurons by transfection with either a scrambled control shRNA exhibiting no homology to any expressed sequence in the rodent genome (Scr), or a previously validated shRNA specifically targeting rodent FGF14 (14KD) (19, 25) and visualized KCNQ2 in the AIS by immunocytochemistry. Neurons transfected with shRNA (Scr or 14KD) were identified by a GFP reporter and the AIS was identified by immunostaining for ank-G. An observer blinded to the shRNA treatment obtained images and quantified the abundance of KCNQ2 by measuring the integrated pixel intensity within the ank-G^+ AIS. In neurons transfected with Scr,

Significance

KCNQ K^+ channels and voltage-gated sodium channels (VGSCs) are both critical determinants of neuronal excitability and highly localized to the axon initial segment (AIS). Although these two classes of ion channels are functionally and spatially linked, information about their coregulation is lacking. Here we report that the VGSC regulator fibroblast growth factor 14 (FGF14) is a regulator of KCNQ channels. FGF14 knockdown in hippocampal neurons leads to loss of KCNQ localization to the AIS and reduced KCNQ currents. Expressed heterologously, FGF14 is a positive regulator of KCNQ channels, ruling out an indirect VGSC-related effect. FGF14 is capable of binding VGSCs and KCNQ2 simultaneously at distinct interaction interfaces, providing a molecular basis for how these channel classes are coregulated in neurons.

Author contributions: J.L.P. and G.S.P. designed research; J.L.P. performed research; J.L.P. contributed new reagents/analytic tools; J.L.P. and G.S.P. analyzed data; and J.L.P. and G.S.P. wrote the paper.

The authors declare no conflict of interest.

This article is a PNAS Direct Submission.

[1]Present address: Cardiovascular Research Institute, Weill Cornell Medicine, New York, NY 10021.

[2]To whom correspondence should be addressed. Email: geoffrey.pitt@med.cornell.edu.

This article contains supporting information online at www.pnas.org/lookup/suppl/doi:10.1073/pnas.1610158114/-/DCSupplemental.

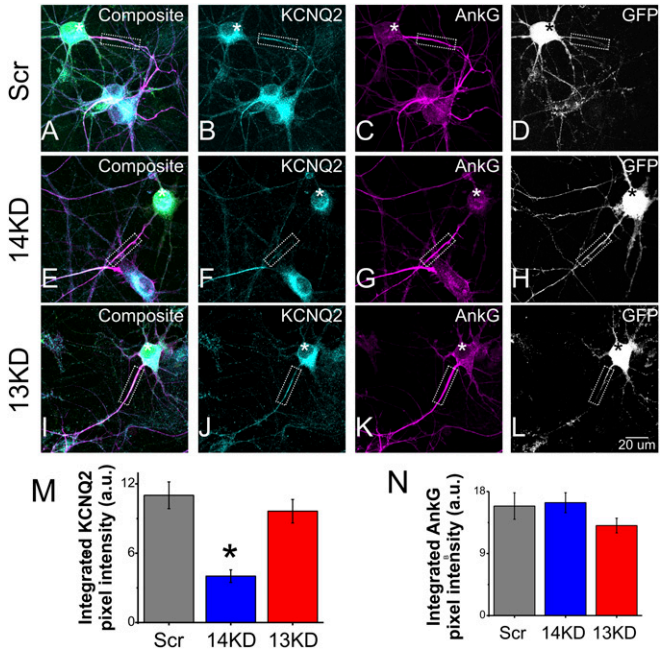

Fig. 1. FGF14 knockdown leads to loss of AIS-localized KCNQ2. (*A–D*) Neurons transfected with scrambled control shRNA (GFP reporter, white signal) exhibit localization of (*B*) KCNQ2 to the AIS as marked by (*C*) ank-G. Nearby untransfected neurons have the same pattern. (*E–H*) Neurons transfected with FGF14-targeted shRNA (GFP reporter, white signal) lose more than half of (*F*) KCNQ2 immunoreactivity at the (*G*) AIS. Nearby untransfected neurons are unaffected. (*I–L*) Neurons transfected with FGF13-targeted shRNA do not exhibit loss of (*J*) KCNQ2 at the (*K*) AIS. (*M*) Quantification of KCNQ2 immunoreactivity via integrated pixel intensity reveals that 14KD but not 13KD significantly reduces KCNQ2 localization compared with Scr. (*N*) Ank-G is not significantly affected across treatments. (*$P < 0.05$; Scr $n = 34$, 14KD $n = 21$, 13KD $n = 40$).

the intensity of KCNQ2 immunoreactivity in the AIS was 99 ± 13% (normalized mean ± error propagated SEM) of the signal in untransfected cells on the same coverslip in the same field of view ($n = 7$ cells in same fields of view), demonstrating that neurons transfected with Scr were indistinguishable from untransfected cells (Fig. 1 *A–D*). In marked contrast, KCNQ2 immunoreactivity in 14KD neurons was reduced by 57 ± 12% ($P < 0.001$) in the AIS (Fig. 1 *E–H* and *M*), whereas KCNQ2 immunoreactivity in the AIS of untransfected neurons on the same coverslip was not different from Scr neurons. There was also a modest 29 ± 11% ($P = 0.03$) decrease in the somatic KCNQ2 signal from 14KD neurons as quantified by integration across equal-area regions of interest (Fig. 1*F*; Scr $n = 12$, 14KD $n = 11$). Because these results were obtained with fully permeabilized neurons, this somatic staining likely reflects KCNQ2 channels in the endomembrane system en route to the AIS in these developing cells. The reduction of AIS-localized KCNQ2 in 14KD neurons was not due to disruption of the AIS, because the intensity and pattern of ank-G immunoreactivity was unchanged (Fig. 1 *G* and *N*). Moreover, the reduction in KCNQ2 appeared to be specific to knockdown of FGF14, because KCNQ2 immunoreactivity was unaffected by knockdown of the homologous FGF13 (Fig. 1 *I–L* and *M*), which is also abundant in hippocampal neurons and concentrated within the AIS (25). Together, these data suggested that FGF14 regulates the localization of KCNQ2 protein in hippocampal neurons, especially within the AIS.

To determine whether FGF14 regulation of KCNQ2 has functional consequences, we analyzed whether FGF14 affected KCNQ2/3 currents in a simplified expression system. When we expressed KCNQ2/3 in human embryonic kidney (HEK) cells with FGF14, we observed an approximate doubling of the K^+ current amplitude at test potentials ≥ −20 mV compared with control cells that were transfected with KCNQ2/3 and empty vector (Fig. 2 *A* and *B*). The voltage dependence of activation was not significantly changed (Fig. 2*C*), suggesting that FGF14 did not alter channel properties (Fig. S1). Rather, using surface biotinylation (Fig. 2*D*), we determined that the amount of surface KCNQ2 is increased in the presence of FGF14, suggesting that the observed increase in currents is likely due to a larger number of KCNQ2 channels at the cell membrane. Further, that FGF14 affects KCNQ2/3 channels in a heterologous expression system makes it unlikely that FGF14 requires a neuronal-specific factor to regulate KCNQ2/3 channels in neurons (Fig. 1).

We therefore tested whether FGF14 knockdown in hippocampal neurons reduced the KCNQ current. To isolate the KCNQ current, we first recorded the basal K^+ current amplitude after blocking voltage-gated Na^+, Ca^{2+}, and Kv1 currents with tetrodotoxin (TTX), Cd^{2+}, and 4-aminopyridine (4-AP) respectively (basal, Fig. 3*A*). We then applied the KCNQ channel blocker, XE-991. Subtracting the remaining current (the XE-991–resistant component) from the basal current gave a XE-991–sensitive current (Fig. 3*A*, *Right*). Analyzing the XE-991–sensitive current showed that the current amplitude obtained after FGF14 knockdown was markedly reduced compared with Scr control (Fig. 3 *B* and *C*), consistent with the reduced KCNQ2 signal by immunocytochemistry observed in the AIS after FGF14 knockdown. The specificity of the effects of FGF14 are highlighted by comparing the consequences of FGF13 knockdown. As shown in Fig. 3 *B* and *C*, knockdown of FGF13 did not affect the KCNQ current. This effect was also consistent with the lack of reduction of KCNQ2 signal in 13KD cells demonstrated by immunocytochemistry (Fig. 1). Focusing on the XE-991–resistant component of the current, it was not significantly affected by

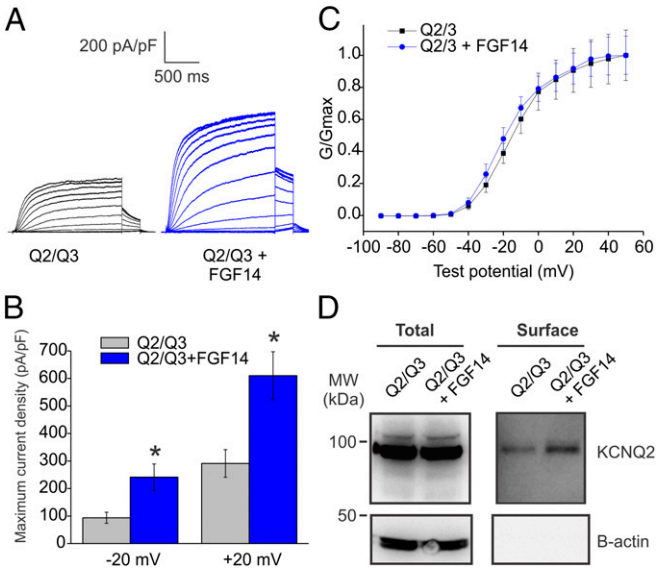

Fig. 2. FGF14 increases KCNQ2/3 current in a heterologous expression system. (*A*) Exemplar K^+ currents from HEK cells transfected with KCNQ2 and KCNQ3 (Q2/Q3) only or with FGF14 added (Q2/Q3 + FGF14). Currents were elicited via a voltage-step protocol in whole-cell voltage clamp. K^+ currents from cells transfected with FGF14 were larger than currents from control cells. (*B*) Maximum current densities from two different test voltages show that the presence of FGF14 promotes larger KCNQ2/3 currents (*$P < 0.05$, $n = 11$, Q2/Q3; $n = 14$, Q2/Q3 + FGF14). (*C*) The $V_{1/2}$ for activation extracted from tail currents (Q2/Q3 = −17.83 ± 2.57 mV, Q2/Q3 + FGF14 = −21.24 ± 2.33 mV; $P = 0.34$) and slope factor (Q2/Q3 = 9.83 ± 0.46 mV, Q2/Q3 + FGF14 = 9.80 ± 0.74 mV; $P = 0.98$) were not significantly changed. (*D*) More KCNQ2 channels are present at the cell membrane when FGF14 is expressed, as revealed by surface biotinylation (representative experiment from three independent trials).

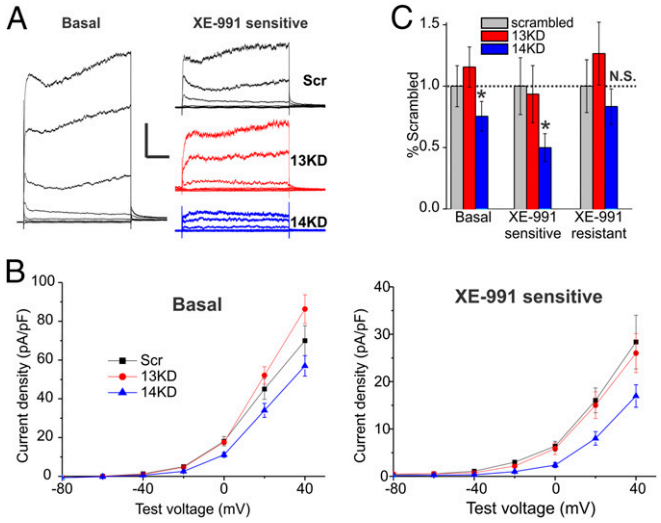

Fig. 3. FGF14 knockdown leads to a decrease in XE-991–sensitive outward currents. (*A*) Currents from DIV10–11 neurons recorded in the presence of TTX, Cd^{2+}, and 4-AP were elicited from a holding potential of −90 mV to steps from −100 mV to 40 mV (*n*, Scr = 16, 14KD = 21, 13KD = 16). KCNQ currents were defined as the noninactivating component of outward potassium current sensitive to 20 μm of XE-991. KCNQ currents from neurons transfected with FGF14-targeted shRNA (14KD) but not FGF13-targeted shRNA (13KD) neurons were smaller than currents from neurons transfected with a scrambled control shRNA (Scr). (Scale bar, 1 nA and 200 ms.) (*B*) Current–voltage relationships plotted for Scr, 13KD, and 14KD. Shown are basal current densities before application of XE-991 and current densities of the XE-991–sensitive component. (*C*) Maximum current amplitudes from the last 100 ms of the 20-mV voltage step were significantly lower for 14KD than for Scr or 13KD. A smaller component of this current was XE-991 sensitive in 14KD neurons, indicating a loss of KCNQ currents. XE-991–resistant currents were not significantly changed although a decremental trend was observed (normalized mean ± error propagated SEM, $*P < 0.05$, ANOVA followed by Fisher's least significant difference (LSD).

14KD, although it did trend down in comparison with Scr and 13KD (Fig. 3*C*). This may indicate that FGF14 can also affect other K^+ channels, although to a lesser degree than for KCNQ channels. In summary, the electrophysiology data from a heterologous expression system and from hippocampal neurons implicate direct regulation of KCNQ2 channels by FGF14, consistent with the reduced amount of KCNQ2 protein observed by immunocytochemistry in hippocampal neurons after FGF14 knockdown (Fig. 1).

We therefore queried the consequences of FGF14 knockdown on integrated neuronal output. Consistent with the observed reduction in KCNQ2/3 K^+ currents, and thus a reduction in voltage-gated K^+ channels open at the resting membrane potential, the input resistance of 14KD neurons was significantly higher than of Scr neurons (Fig. 4*A*). Further, the resting membrane potential of 14KD neurons was also more depolarized than for Scr neurons (Scr = −55.0 ± 1.1 mV, 14KD = −51.8 ± 0.8 mV, $P < 0.05$; Scr $n = 12$, 14KD $n = 15$). A loss of repolarization was also suggested by two other observations. First, we observed a larger amplitude rise in interspike voltage during the course of a 500-ms current injection for 14KD neurons than for Scr neurons (Fig. 4 *B* and *C*). Second, during action potential trains initiated by current injection, we noted an increase in the voltages for threshold of subsequent action potentials in 14KD neurons, even though the threshold voltage for the first action potential was unchanged (Fig. 4*D*). Finally, with current injections of increasing amplitude, fewer action potentials were elicited from 14KD neurons than from Scr control neurons (Fig. 4*E*), in agreement with previous work on FGF14 loss-of-function models (18, 22). Thus, FGF14 knockdown in neurons results in changes in passive membrane properties as well as excitability that can be explained by alterations to both potassium and sodium currents.

We reasoned that FGF14 regulation of KCNQ2/3 might be mediated by a previously unrecognized FGF14 interaction with the KCNQ2/3 complex and tested this hypothesis by immunoprecipitating FGF14 from HEK cells transfected with KCNQ2, FGF14, or both. Immunoprecipitation (IP) of FGF14 coprecipitated KCNQ2 only when FGF14 was cotransfected (Fig. 5*A*). In contrast, the two most abundant isoforms of FGF13 did not exhibit an interaction with KCNQ2 (Fig. 5*B*), consistent with the lack of an effect on KCNQ2 localization and function after FGF13 knockdown (Figs. 1 and 3). Thus, the regulation of KCNQ2/3 by FGF14 is likely due to a previously unrecognized interaction between FGF14 and KCNQ2.

Having established KCNQ2 as an interacting partner of FGF14, we sought to delineate the FGF14 binding determinants on KCNQ2. First, we tested for direct interaction between FGF14 and a KCNQ2 C-terminal domain (CTD) construct (amino acids 319–658), hypothesizing parallels with VGSCs (26, 27), the best-characterized FHF binding partners. The FHF interaction site in VGSCs is on the intracellular CTD adjacent to a calmodulin binding site and the KCNQ2 CTD also contains a calmodulin binding site (28–31). We therefore tested whether an untagged recombinant FGF14 (amino acids 70–252) copurified with a coexpressed 6xHis-tagged recombinant KCNQ2 C terminus construct and recombinant calmodulin. Whereas calmodulin copurified with the 6xHis-tagged KCNQ2 C terminus on a metal affinity column, FGF14 did not (Fig. 6*A*, *Left*). We also tested another CTD construct (amino acids 626–876) with similar results (Fig. 6*A*, *Right*). This construct did not have the IQ motif for CaM binding and, as expected, did not significantly copurify CaM. Having eliminated the KCNQ2 CTD as a direct FGF14 binding determinant, we performed the converse experiment and tested whether FGF14 bound to a KCNQ2 construct in which the C terminus was deleted (KCNQ2ΔCTD). We expressed both FGF14 and KCNQ2ΔCTD in HEK cells and immunoprecipitated FGF14. Indeed, the KCNQ2ΔCTD still coimmunoprecipitated, indicating that the KCNQ2 CTD is not

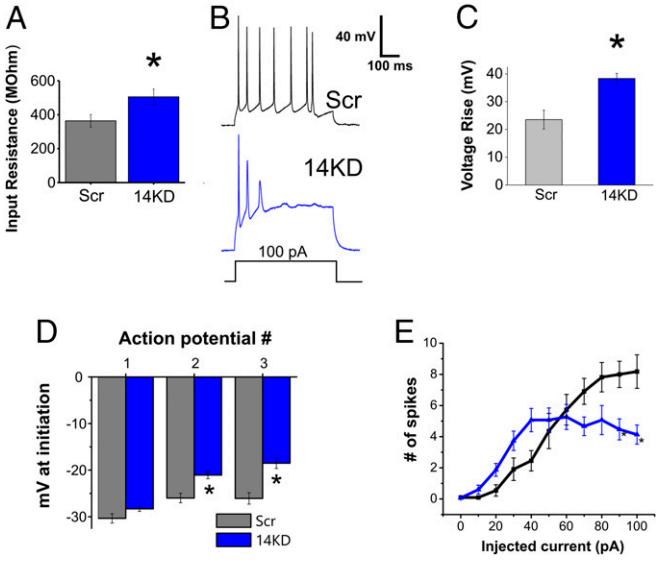

Fig. 4. FGF14 knockdown changes intrinsic membrane properties and action potential generation. (*A*) The input resistance of 14KD neurons is higher than for Scr neurons. (*B*) Examples of action potential trains generated from 100-pA injections into both Scr and 14KD neurons. In 14KD neurons, the rise in interspike voltage during the current injection step is higher. Quantification is shown in *C*. (*D*) The threshold for action potentials subsequent to the first action potential of a train is higher in 14KD neurons than it is in Scr control neurons. (*E*) Increasing current injections lead to decreased numbers of action potentials generated from 14KD neurons compared with Scr neurons. ($*P < 0.05$, Student's *t* test; $n = 11$–15 cells each).

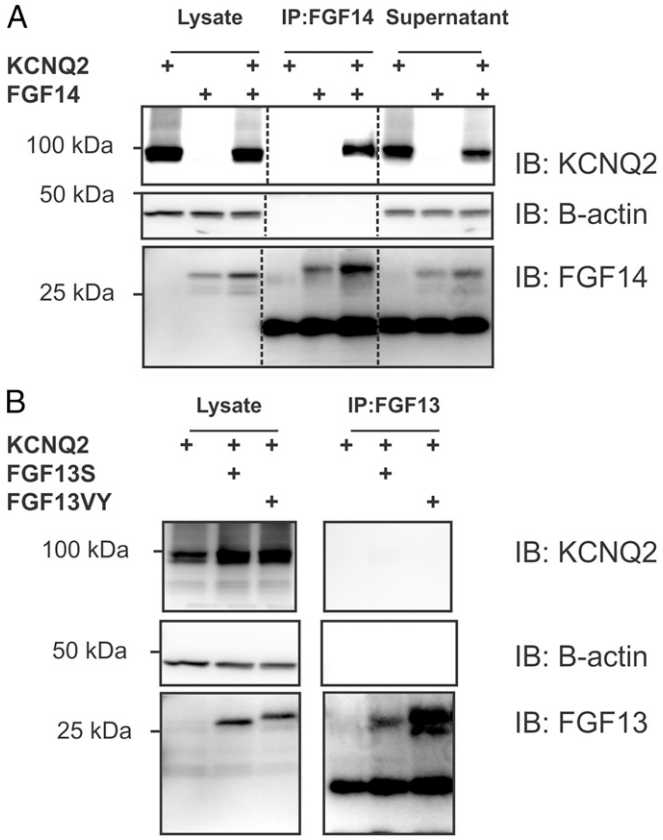

Fig. 5. FGF14 but not FGF13 binds to KCNQ2. (*A*) Coimmunoprecipitation experiments with heterologous expression of KCNQ2 and FGF14 show that immunoprecipitating FGF14 leads to the coimmunoprecipitation of KCNQ2. This result is not true when one of these proteins is omitted. KCNQ2 signal is decreased in input material (supernatant) only when FGF14 is present and immunoprecipitated, again indicating binding (representative experiment from four independent trials). Dark bands below the FGF14 bands are IgG from the antibodies used for the IP. (*B*) Immunoprecipitation of FGF13 (splice variants FGF13S or FGF13VY) leads to no discernible signal for coimmunoprecipitation of KCNQ2. This finding indicates that FGF13 does not bind to KCNQ2 (representative experiment from three independent trials). Dark bands below the FGF13 bands are IgG from the antibodies used for the IP.

necessary for interaction with FGF14 (Fig. 6*B*). To further analyze a specific KCNQ2 intracellular domain(s) contributing to a possible direct interaction, we coexpressed the KCNQ2 N terminus with FGF14. Immunoprecipitation of FGF14, however, did not coimmunoprecipitate the KCNQ2 N terminus, although the full-length KCNQ2 was immunoprecipitated (Fig. 6*C*). Thus, FGF14 binding requires the smaller intracellular loops, interactions among multiple domains, or a mediator protein.

Because sequence analysis of those KCNQ2 intracellular domains did not reveal any clear homology to the identified FHF binding site in VGSC CTDs, we hypothesized that the mode of binding between FGF14 and KCNQ2 differed from how FGF14 and VGSCs interact and, consequently, the binding determinants on FGF14 would be distinct between KCNQ2 and VGSCs. Our structural analyses that had identified the VGSC binding surface on FGF14 (27) had previously shown that direct interaction between FGF14 and VGSCs could be disrupted when an exposed arginine residue in FGF14 (R117 in FGF14B) was mutated to an alanine (21). We therefore assessed whether immunoprecipitation of an R117A-mutant FGF14 ($FGF14^{RA}$) coprecipitated KCNQ2. As we previously showed, immunoprecipitation of $FGF14^{RA}$ was incapable of coprecipitating $Na_V1.6$. In stark contrast, however, immunoprecipitation of $FGF14^{RA}$ coprecipitated KCNQ2 (Fig. 7). This finding indicated separate interaction surfaces on FGF14 for binding VGSCs and KCNQ2.

Distinct interaction surfaces for VGSCs and KCNQ2 on FGF14 implied that FGF14 might bind these two ion channels simultaneously, thereby providing a basis for KCNQ2/3 regulation of VGSC currents (14). To test this hypothesis, we coexpressed KCNQ2 and the VGSC $Na_V1.6$ in the presence or absence of FGF14 and observed whether $Na_V1.6$ coimmunoprecipitated with KCNQ2. Indeed, $Na_V1.6$ coimmunoprecipitated with KCNQ2 only in the presence of FGF14 (Fig. 8). Together, these data indicated that FGF14 could bridge these two axonal ion channels.

Discussion

This report shows that FHFs regulate voltage-gated K^+ channels. Although originally described as VGSC modulators, FHFs have increased their regulatory portfolios, recently shown to include voltage-gated Ca^{2+} channels and now K^+ channels. We hypothesize that this FHF-dependent regulation of multiple ion channels is a mechanism for coordinating and integrating various ionic conductances. For example, regulation of KCNQ2 and VGSCs

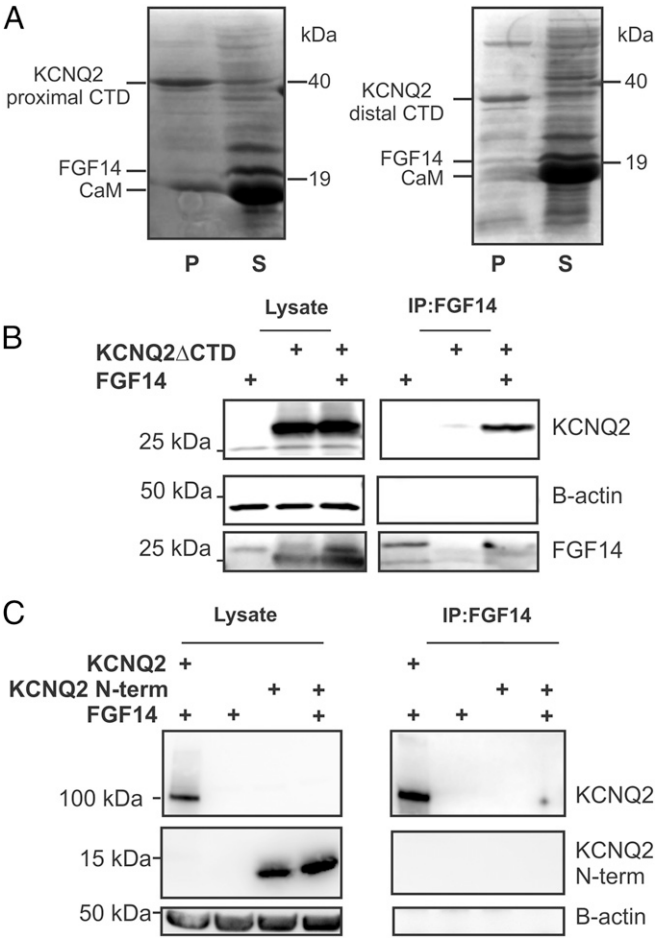

Fig. 6. FGF14 binding to KCNQ2 does not require the C terminus nor is the KCNQ2 N terminus sufficient for binding. (*A*) Copurification experiments with a 6xHis-tagged KCNQ2 C terminus show that calmodulin (CaM) binds, whereas FGF14 does not. A different KCNQ2 C terminus construct, without the CaM binding site, copurifies neither FGF14 nor CaM. (*B*) Immunoprecipitation of FGF14 is still capable of immunoprecipitating a KCNQ2 construct that lacks a C terminus. Omission of either protein does not yield a significant signal. (*C*) Immunoprecipitation of FGF14 does not coimmunoprecipitate HA-tagged KCNQ2 N terminus. Coimmunoprecipitation of the full-length HA-tagged KCNQ2 is shown as a positive control.

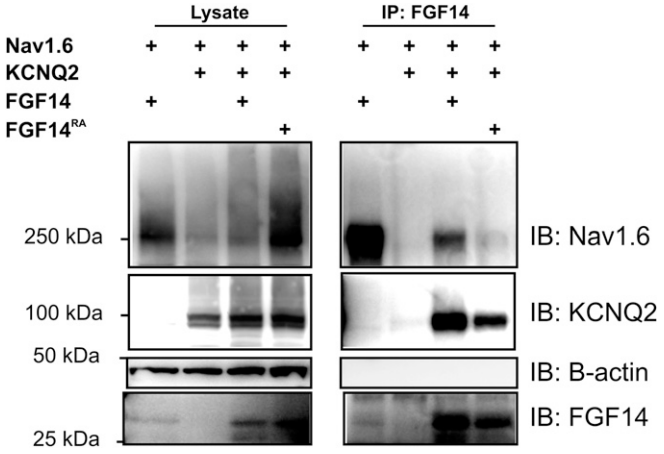

Fig. 7. FGF14 binds to KCNQ2 at an interface distinct from Na_V binding. Immunoprecipitation of wild-type FGF14 coimmunoprecipitates both $Na_V1.6$ and KCNQ2. In contrast, immunoprecipitation of a Na_V binding-deficient $FGF14^{RA}$ mutant does not coimmunoprecipitate $Na_V1.6$, but still retains the capability to coimmunoprecipitate KCNQ2 (representative experiment from three independent trials).

within the AIS—where FGF14, KCNQ2, and VGSCs are concentrated—along with the observation that FGF14 bridges KCNQ2 and VGSCs provide context to recent data showing how KCNQ2/3 channels within the axon coordinate with VGSCs to control membrane potential (14). In that study, inhibition of KCNQ currents depolarized resting membrane potential because of loss of a counterbalance to the persistent inward current through VGSCs. Here, we observed that FGF14 knockdown and a resulting reduction in KCNQ2/3 currents were also associated with a slight but significant depolarization in resting membrane potential. Such an effect could not solely be predicted by previously reported FGF14-mediated reduction in VGSC currents (25), which would diminish the contribution of the opposing persistent VGSC current (21), because that result would lead to hyperpolarization. Thus, the direct effects we observed upon KCNQ currents after FGF14 knockdown suggest significant regulation of KCNQ channels.

Adding support to this concept that FGF14 exerts its effects through concerted regulation of multiple ionic conductances are comparisons with previous studies of KCNQ inhibition in central nervous system neurons. The resulting effects after KCNQ inhibition (14, 32) are distinct from what we observed here after FGF14 knockdown. For example, inhibition of the M current with bath application of XE-991 produced more spikes with a given current injection. With FGF14 knockdown, however, we observed a rise in membrane potential and input resistance consistent with M-current inhibition, but we also observed decreases in spike frequency with current injection (Fig. 4). Specifically, we hypothesize that these differences result from FGF14 regulation of VGSCs as well as KCNQ2. Decreased excitability after current injection was previously reported for FGF14 loss of function (20, 24) and was attributed to a loss of FGF14 regulation of VGSCs. Here we highlight additional effects of silencing FGF14, namely an increase in the baseline voltage over an action potential train, which indicate additional effects on repolarizing currents.

Neurons deficient in FGF14 are less excitable, previously attributed to loss of function of VGSCs. Our results, using acute FGF14 knockdown that obviates any compensatory changes resultant from an embryonic knockout, offer an additional mechanism in that FGF14 deficiency also leads to a loss of function in KCNQ2/3 currents. In a previous study in cerebellar Purkinje neurons, action potential firing was impaired and the voltage dependence of steady-state VGSC inactivation was hyperpolarized after acute FGF14 knockdown (23). Hyperpolarizing injections restored repetitive firing, indicating the importance of membrane potential. As we showed here, FGF14 knockdown leads to the loss of repolarizing drive due to decreased KCNQ2/3 K^+ current amplitude. Thus, the excitability deficits in 14KD neurons (Fig. 4), in animal models of *Fg14* ablation (24, 33), or in patients with *FGF14* mutations associated with SCA27 (17, 18), likely result from the multiple effects of loss of FGF14.

Structural and biochemical characterization of the scaffolding molecule ank-G has shown that the ANK repeat domain contains several target binding sites (9). In agreement with this finding, Xu and Cooper reported that the modes of Na_V and KCNQ2/3 binding to ank-G differ from each other (10). Thus, our work contributes to a broadening picture of the intricate molecular arrangements that define AIS organization. FGF14 knockdown does not affect ank-G (Fig. 1) but ank-G knockdown does abolish AIS localization of FGF14 (25). FGF14, therefore, is likely to function downstream of ank-G in ensuring proper localization of Na_V and KCNQ2/3 at the AIS. The regulatory roles of FGF14 and ank-G are unlikely to be redundant because FGF14 knockdown affects these ion channels even with ank-G present; therefore, it is possible that FGF14 and ank-G are complementary or reinforcing in their regulation of AIS channels.

Our biochemical analyses provide footprints for the interacting sites on FGF14 and on KCNQ2. First, the $FGF14^{RA}$ mutant on the VGSC interaction surface, which coprecipitated with KCNQ2 but not with $Na_V1.6$, demonstrates that the interaction determinants on FGF14 for KCNQ2 are different from for VGSCs. Thus, the well-characterized VGSC CTD interaction surface on FHFs (22, 27) can be excluded. The demonstration that FGF14 can bind $Na_V1.6$ and KCNQ2 simultaneously (Fig. 8) further points to an alternative interaction surface on FGF14. The globular nature of the FGF-like core domain in FGF14 provides several faces that remain unencumbered by an interaction with a VGSC. Within KCNQ2, we were able to eliminate about half of the protein—and even more of the intracellular domains—by demonstrating that a KCNQ2 channel devoid of its C terminus (KCNQ2ΔCTD) was still able to coprecipitate with FGF14 (Fig. 6*B*). Remaining candidate interaction sites within KCNQ2 include the small loops between transmembrane segments S2–S3 or S4–S5. It is also possible that the binding site for FGF14 consists of multiple domains or that there is a nonneuronal-specific mediator protein between FGF14 and KCNQ2.

The decreased current amplitude of neuronal KCNQ channels (Fig. 3) after FGF14 knockdown is likely through a mechanism by which FGF14 regulates KCNQ2/3 surface expression, as indicated by surface biotinylation experiments (Fig. 2). In addition,

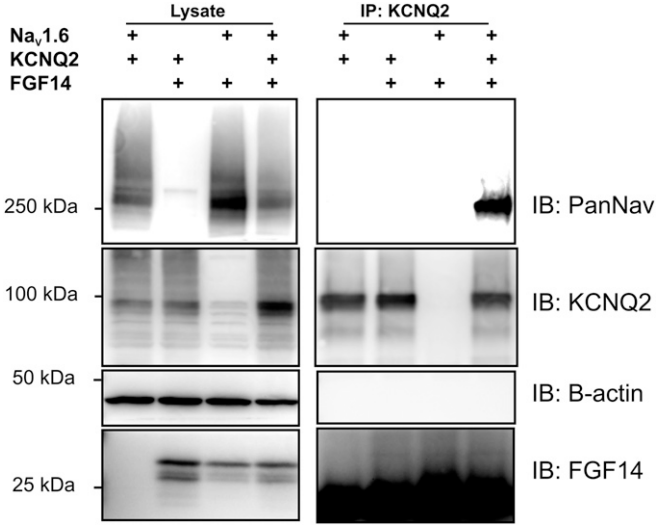

Fig. 8. FGF14 bridges $Na_V1.6$ and KCNQ2. Immunoprecipitation of KCNQ2 is only capable of coimmunoprecipitating $Na_V1.6$ in the presence of FGF14. Omission of any of these three components leads to no signal (representative experiment from three independent trials).

FGF14 may help localize KCNQ2 in the AIS, as we observed a significant reduction of KCNQ2 signal in the AIS after FGF14 knockdown (Fig. 1). Surface expression and current amplitude are not always correlated (34) but we find that FGF14 affects both parameters similar to what we previously showed for Na_V channels (25). In this context, it would be interesting to explore whether VGSCs and KCNQ2 are coupled in their trafficking and localization at particular stages in neuronal development and whether FGF14 plays a role in such a process. Such a result would be consistent with recent evidence suggesting coregulation of members of the KCNQ and VGSC families (35).

Materials and Methods

Primary Hippocampal Culture and Transfection. Primary dissociated hippocampal cultures were prepared as described (37), with minor modifications. After 5 d in vitro (DIV) culture, the neurons were transiently transfected with 0.2 μg plasmid DNA per coverslip using Lipofectamine 2000 (Invitrogen), according to the manufacturer's instructions.

Immunocytochemistry and Quantification. Cultured hippocampal cells were fixed with 2% (vol/vol) paraformaldehyde, blocked, and permeabilized with 5% (vol/vol) fish skin gelatin, 0.1% Triton X-100 in PBS. Antibodies used were Thermo rabbit anti-KCNQ2 PA1-929 (1:200) and polyclonal goat anti–ank-G (1:1,000, gift from V. Bennett, Duke University, Durham, NC). Imaging was performed with a Zeiss LSM 780 confocal microscope using an oil immersion 63× objective. Quantification using NIH ImageJ software was performed based on the methods of Grubb and Burrone (38). In all image analysis, the experimenter was blinded to the identity of the confocal channels.

Western Blotting and Immunoprecipitation. Cells were lysed with 150 mM NaCl, 50 mM Tris, 1% sodium deoxycholate, and 1% Triton X-100. Homogenized proteins were incubated with primary antibodies overnight and immunoprecipitated with Protein A/G beads. Samples were run on Tris-glycine SDS/PAGE gels and transferred to PVDF membranes.

Biotinylation. Transfected cells were biotinylated with 1 mg/mL EZ-Link Sulfo NHS-SS Biotinylation (Pierce) in cold PBS, then pulled down with NeutrAvidin beads (Pierce).

Electrophysiological Recordings. Whole-cell voltage or current clamp recordings were obtained from cultured hippocampal cells or HEK 293T cells using an Axopatch 200B amplifier (Axon Instruments), with a 5-kHz bandwidth filter.

Molecular Biology. The shRNA sequences targeting both FGF14 and FGF13 were cloned into the pLVTHM plasmid (Addgene) and have been described previously (19, 25, 39).

ACKNOWLEDGMENTS. We thank James Wu (Duke University) for help with protein expression.

1. Lai HC, Jan LY (2006) The distribution and targeting of neuronal voltage-gated ion channels. *Nat Rev Neurosci* 7(7):548–562.
2. Vacher H, Trimmer JS (2012) Trafficking mechanisms underlying neuronal voltage-gated ion channel localization at the axon initial segment. *Epilepsia* 53(Suppl 9): 21–31.
3. Devaux JJ, Kleopa KA, Cooper EC, Scherer SS (2004) KCNQ2 is a nodal K+ channel. *J Neurosci* 24(5):1236–1244.
4. Zhou D, et al. (1998) AnkyrinG is required for clustering of voltage-gated Na channels at axon initial segments and for normal action potential firing. *J Cell Biol* 143(5): 1295–1304.
5. Catterall WA (1981) Localization of sodium channels in cultured neural cells. *J Neurosci* 1(7):777–783.
6. Jenkins PM, et al. (2015) Giant ankyrin-G: A critical innovation in vertebrate evolution of fast and integrated neuronal signaling. *Proc Natl Acad Sci USA* 112(4):957–964.
7. Hedstrom KL, Ogawa Y, Rasband MN (2008) AnkyrinG is required for maintenance of the axon initial segment and neuronal polarity. *J Cell Biol* 183(4):635–640.
8. Pan Z, et al. (2006) A common ankyrin-G-based mechanism retains KCNQ and NaV channels at electrically active domains of the axon. *J Neurosci* 26(10):2599–2613.
9. Wang C, et al. (2014) Structural basis of diverse membrane target recognitions by ankyrins. *eLife* 3:3.
10. Xu M, Cooper EC (2015) An Ankyrin-G N-terminal gate and protein kinase CK2 dually regulate binding of voltage-gated sodium and KCNQ2/3 potassium channels. *J Biol Chem* 290(27):16619–16632.
11. Cavaretta JP, et al. (2014) Polarized axonal surface expression of neuronal KCNQ potassium channels is regulated by calmodulin interaction with KCNQ2 subunit. *PLoS One* 9(7):e103655.
12. Liu W, Devaux JJ (2014) Calmodulin orchestrates the heteromeric assembly and the trafficking of KCNQ2/3 (Kv7.2/3) channels in neurons. *Mol Cell Neurosci* 58:40–52.
13. Chung HJ, Jan YN, Jan LY (2006) Polarized axonal surface expression of neuronal KCNQ channels is mediated by multiple signals in the KCNQ2 and KCNQ3 C-terminal domains. *Proc Natl Acad Sci USA* 103(23):8870–8875.
14. Battefeld A, Tran BT, Gavrilis J, Cooper EC, Kole MH (2014) Heteromeric Kv7.2/7.3 channels differentially regulate action potential initiation and conduction in neocortical myelinated axons. *J Neurosci* 34(10):3719–3732.
15. Smallwood PM, et al. (1996) Fibroblast growth factor (FGF) homologous factors: New members of the FGF family implicated in nervous system development. *Proc Natl Acad Sci USA* 93(18):9850–9857.
16. Lou JY, et al. (2005) Fibroblast growth factor 14 is an intracellular modulator of voltage-gated sodium channels. *J Physiol* 569(Pt 1):179–193.
17. van Swieten JC, et al. (2003) A mutation in the fibroblast growth factor 14 gene is associated with autosomal dominant cerebellar ataxia [corrected]. *Am J Hum Genet* 72(1):191–199.
18. Dalski A, et al. (2005) Mutation analysis in the fibroblast growth factor 14 gene: Frameshift mutation and polymorphisms in patients with inherited ataxias. *Eur J Hum Genet* 13(1):118–120.
19. Yan H, Pablo JL, Pitt GS (2013) FGF14 regulates presynaptic Ca2+ channels and synaptic transmission. *Cell Reports* 4(1):66–75.
20. Laezza F, et al. (2007) The FGF14(F145S) mutation disrupts the interaction of FGF14 with voltage-gated Na+ channels and impairs neuronal excitability. *J Neurosci* 27(44): 12033–12044.
21. Yan H, Pablo JL, Wang C, Pitt GS (2014) FGF14 modulates resurgent sodium current in mouse cerebellar Purkinje neurons. *eLife* 3:e04193.
22. Wang C, et al. (2014) Structural analyses of Ca^{2+}/CaM interaction with NaV channel C-termini reveal mechanisms of calcium-dependent regulation. *Nat Commun* 5:4896.
23. Bosch MK, et al. (2015) Intracellular FGF14 (iFGF14) is required for spontaneous and evoked firing in cerebellar Purkinje neurons and for motor coordination and balance. *J Neurosci* 35(17):6752–6769.
24. Goldfarb M, et al. (2007) Fibroblast growth factor homologous factors control neuronal excitability through modulation of voltage-gated sodium channels. *Neuron* 55(3):449–463.
25. Pablo JL, Wang C, Presby MM, Pitt GS (2016) Polarized localization of voltage-gated Na+ channels is regulated by concerted FGF13 and FGF14 action. *Proc Natl Acad Sci USA* 113(19):E2665–E2674.
26. Wang C, Wang C, Hoch EG, Pitt GS (2011) Identification of novel interaction sites that determine specificity between fibroblast growth factor homologous factors and voltage-gated sodium channels. *J Biol Chem* 286(27):24253–24263.
27. Wang C, Chung BC, Yan H, Lee SY, Pitt GS (2012) Crystal structure of the ternary complex of a NaV C-terminal domain, a fibroblast growth factor homologous factor, and calmodulin. *Structure* 20(7):1167–1176.
28. Yus-Najera E, Santana-Castro I, Villarroel A (2002) The identification and characterization of a noncontinuous calmodulin-binding site in noninactivating voltage-dependent KCNQ potassium channels. *J Biol Chem* 277(32):28545–28553.
29. Wen H, Levitan IB (2002) Calmodulin is an auxiliary subunit of KCNQ2/3 potassium channels. *J Neurosci* 22(18):7991–8001.
30. Gamper N, Shapiro MS (2003) Calmodulin mediates Ca2+-dependent modulation of M-type K+ channels. *J Gen Physiol* 122(1):17–31.
31. Xu Q, Chang A, Tolia A, Minor DL, Jr (2013) Structure of a Ca(2+)/CaM:Kv7.4 (KCNQ4) B-helix complex provides insight into M current modulation. *J Mol Biol* 425(2): 378–394.
32. Shah MM, Migliore M, Valencia I, Cooper EC, Brown DA (2008) Functional significance of axonal Kv7 channels in hippocampal pyramidal neurons. *Proc Natl Acad Sci USA* 105(22):7869–7874.
33. Wang Q, et al. (2002) Ataxia and paroxysmal dyskinesia in mice lacking axonally transported FGF14. *Neuron* 35(1):25–38.
34. Choveau FS, Shapiro MS (2012) Regions of KCNQ K(+) channels controlling functional expression. *Front Physiol* 3:397.
35. Rannals MD, et al. (2016) Psychiatric risk gene transcription factor 4 regulates intrinsic excitability of prefrontal neurons via repression of SCN10a and KCNQ1. *Neuron* 90(1): 43–55.
36. Goetz R, et al. (2009) Crystal structure of a fibroblast growth factor homologous factor (FHF) defines a conserved surface on FHFs for binding and modulation of voltage-gated sodium channels. *J Biol Chem* 284(26):17883–17896.
37. Wang HG, George MS, Kim J, Wang C, Pitt GS (2007) Ca2+/calmodulin regulates trafficking of Ca(V)1.2 Ca2+ channels in cultured hippocampal neurons. *J Neurosci* 27(34):9086–9093.
38. Grubb MS, Burrone J (2010) Activity-dependent relocation of the axon initial segment fine-tunes neuronal excitability. *Nature* 465(7301):1070–1074.
39. Wang C, et al. (2011) Fibroblast growth factor homologous factor 13 regulates Na+ channels and conduction velocity in murine hearts. *Circ Res* 109(7):775–782.